Matter from light-light scattering via Breit-Wheeler events produced by two interacting Compton sources

Illya Drebot,[1] D. Micieli,[2,3] E. Milotti,[4] V. Petrillo,[5,1] E. Tassi,[2,3] and L. Serafini[1]

[1]*INFN-Sezione di Milano, via Celoria 16, 20133 Milano, Italy*
[2]*Università degli Studi della Calabria, Arcavacata di Rende (Cosenza), Italy*
[3]*INFN-Sezione di Cosenza, Arcavacata di Rende (Cosenza), Italy*
[4]*Università di Trieste and INFN-Sezione di Trieste, Via Valerio 2, 34127 Trieste, Italy*
[5]*Università degli Studi di Milano, via Celoria 16, 20133, Milano, Italy*

(Received 24 December 2016; published 26 April 2017)

We present the dimensioning of a photon-photon collider based on Compton gamma sources for the observation of Breit-Wheeler pair production and QED $\gamma\gamma$ events. Two symmetric electron beams, generated by photocathodes and accelerated in linacs, produce two gamma ray beams through Compton back scattering with two J-class lasers. Tuning the system energy above the Breit-Wheeler cross section threshold, a flux of electron-positron pairs is generated out of light-light interaction. The process is analyzed by start-to-end simulations. Realistic numbers of the secondary particle yield, referring to existing state-of-the-art set-ups and a discussion of the feasibility of the experiment taking into account the background signal are presented.

DOI: 10.1103/PhysRevAccelBeams.20.043402

I. INTRODUCTION

The recent development of high-energy, high-brilliance photon pulses and high-brightness electron beams opens the way to the study of quantum electrodynamics (QED) processes so far unobserved or detected only in indirect way. Light-light interaction is a most elusive QED phenomenon, which can lead to the Breit-Wheeler pair production (BWPP, $\gamma\gamma \to e^-e^+$) [1] or to the $\gamma\gamma \to \gamma\gamma$ elastic scattering and higher-order processes: implied by Dirac's theory of the electrons and studied since the early thirties, none of them has been yet directly measured. Present experiments aimed at detecting the elastic $\gamma\gamma$ scattering operate at low energies and therefore deal with very demanding challenges due to the exceedingly low values of the interaction cross-section at these energy values (see, e.g., [2,3]). Although the performance of the experiments has gradually improved and the goal of a direct observation looks no longer so distant [2], a first detection has not yet been achieved. The process, however, has been observed as a radiative correction in Compton scattering of photons off nuclei [4], and there is a very recent claim that points to it as the main responsible of the unexpectedly high linear polarization of the light coming from the isolated neutron star RX J1856.5–3754 [5]. BWPP—the simplest mechanism by which light converts to matter—has a much higher cross-section, but nevertheless it has never been observed to this date as well. Several different experimental schemes have been proposed [6–11], but not a single one has been so far implemented, apart from the experiment of Burke *et al.*, which detected the more complex multiphoton Breit-Wheeler process almost twenty years ago [12]. Advanced Compton sources generating hard X and gamma radiation [13], presently in construction, will permit us to reach and explore the center of mass energy region around 1–2 MeV and more, close to the peak of the elastic $\gamma\gamma$ scattering and just beyond the threshold of BWPP, pointing the way for the realization of a true photon-photon collider with the advent of a new generation of high-energy physics experiments. Other QED collisions such as secondary Compton ($e^-\gamma \to e^-\gamma$), Møller scattering ($e^-e^- \to e^-e^-$), triplet pair (TPP, $\gamma e^- \to e^-e^+e^-$), and muon pair photo-production (MPP, $\gamma e^- \to e^-\mu^+\mu^-$) also take place in this framework because of collisions between the primary electron beams and the Compton back-scattered photons. These processes produce a potentially interfering background, but they can be discriminated thanks to their angular distributions which are different from those of elastic $\gamma\gamma$ scattering and BWPP; they are also an interesting source of particle-antiparticle pairs. In Ref. [14] we presented an analysis of $\gamma\gamma$ elastic scattering and the dimensioning of a $\gamma\gamma$ collider based on Compton gamma sources. To this aim, a code named ROSE (rate of scattering events) was developed [15] and benchmarked with respect to the particle-in-cell code CAIN [16] for Compton emission [17].

In this paper, we analyze the Breit-Wheeler pair production from the collision of two gamma-ray beams generated by state-of-the-art Compton sources. The scheme of the source is shown in Fig. 1 and presents the clear advantage of a rather clean environment due to the absence of high-Z materials in

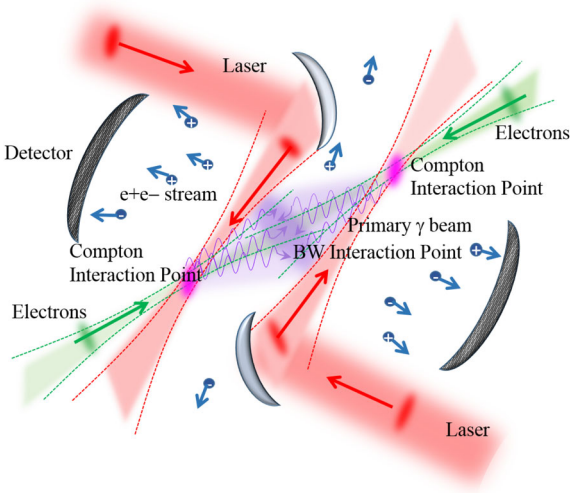

FIG. 1. Scheme of the BW interaction.

the proximity of the interaction region. We study and optimize the rate of events in situations where the experimental parameters are not particularly demanding and not requiring performances beyond the state of the art. The total number of events, even though not as large as in Ref. [11], should permit the detection of BWPP in a short time and with fairly good statistics. We also show that the background from TPP, Møller, and Compton scattering, that we quantify and discuss, is not a limiting factor in measurements of BWPP.

II. KINEMATICS AND CROSS SECTION OF THE BREIT-WHEELER SCATTERING

The evaluation of the rate of particle production first requires the determination of the phase space of the reaction products. The generic binary reaction $(12 \to 34)$ is usually analyzed in the center of mass reference frame (CM) where, giving the invariant mass $\sqrt{s} = \sqrt{m_1^2 + m_2^2 + 2(E_1E_2 - \underline{p}_1 \cdot \underline{p}_2)}$ (E_1, E_2 being the energies of two primary particles with momenta, in natural units, respectively $\underline{p}_1$ and $\underline{p}_2$ in the laboratory and $c = 1$), the final state particles 3 and 4 acquire the energies $E_{3,4}^{\mathrm{CM}} = (s + m_{3,4}^2 - m_{4,3}^2)/(2\sqrt{s})$, with momenta $\underline{p}_3^{\mathrm{CM}} = -\underline{p}_4^{\mathrm{CM}}$, equal in modulus, directed at angles $\theta_3^{\mathrm{CM}} = \pi - \theta_4^{\mathrm{CM}}$ and $\varphi_3^{\mathrm{CM}} = \pi + \varphi_4^{\mathrm{CM}}$.

Customary Monte Carlo strategies for analyzing the problem rely on the random sampling of the angles φ_4^{CM} and θ_4^{CM} followed by the acceptance-rejection method weighted by the differential cross-section $d\sigma/d\Omega$.

The last step is the Lorentz transformation back to the laboratory system with the determination of $\underline{p}_{3,4}$ and $E_{3,4}$.

In the case of BWPP, the incoming particles are photons $(m_1 = m_2 = 0)$, while the generated particles have the same mass $m_{3,4} = m_e$, and, therefore, they simply share the energy $E_{3,4}^{\mathrm{CM}} = \sqrt{s}/2$.

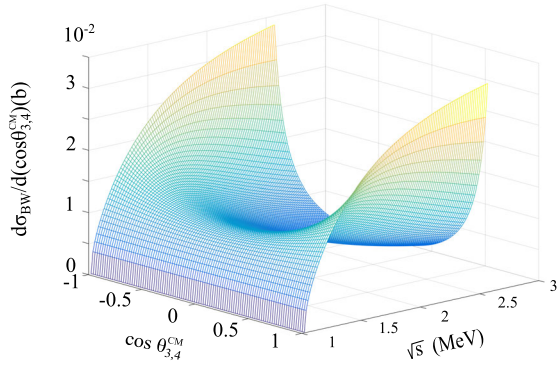

FIG. 2. Differential cross section $d\sigma_{\mathrm{BW}}/d(\cos\theta_{3,4}^{\mathrm{CM}})$ averaged on the angle $\phi_{3,4}^{\mathrm{CM}}$ for Breit-Wheeler scattering in the plane $(\sqrt{s}, \theta_{3,4}^{\mathrm{CM}})$.

The Breit-Wheeler differential cross-section can be deduced by means of the substitution rule from the Klein-Nishina one. According to it, for unpolarized photons, we have:

$$\frac{d\sigma_{\mathrm{BW}}}{d\Omega} = \frac{r_0^2\beta}{s}\left[\frac{1 + 2\beta^2\sin^2\theta_{\mathrm{CM}} - \beta^4 - \beta^4\sin^4\theta_{\mathrm{CM}}}{(1 - \beta^2\cos^2\theta_{\mathrm{CM}})^2}\right] \quad (1)$$

with r_0 the electron classical radius and $\beta = \sqrt{1 - 4m_e^2/s}$, resulting in the shape of Fig. 2. The cross-section presents a threshold at $\sqrt{s} = 2m_e$.

The total cross-sections of all the involved processes are reported in Fig. 3 as functions of the relevant center of mass energy $\sqrt{s}$.

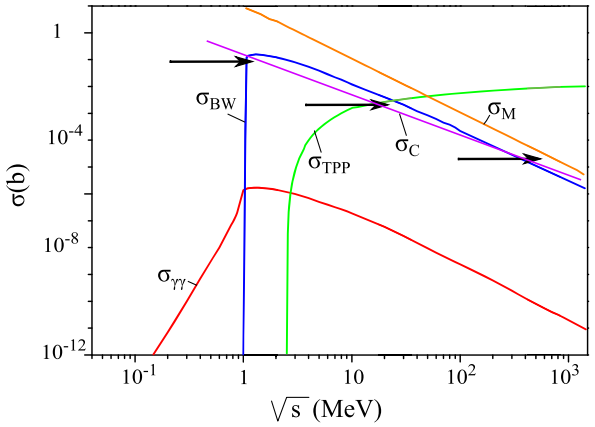

FIG. 3. Total cross section in b for gamma gamma ($\sigma_{\gamma\gamma}$, red line), Breit-Wheeler (σ_{BW}, blue line), TPP (σ_{TPP}, green line), Møller (σ_M, orange line) and Compton (violet line) scatterings versus the energy in the center of mass $\sqrt{s}$ (in MeV) of each process. In blue, green, and orange the center of mass energy regions involved in the various processes for electron energy of about 260 MeV. The arrows mark the values of the cross-sections. The Møller cross-section has been evaluated with a cut at $|\cos\theta| < 0.999$.

TABLE I. Table of electron beam and laser parameters.

Electron parameters		Laser parameters	
Electron energy (MeV)	260	Laser wavelength μm	1
Electron charge (pC)	250	Laser energy (J)	2
Transverse size (μm)	5	Waist (μm)	10
Longitudinal size (μm)	400	Longitudinal size (mm)	1
Emittance (mm mrad)	0.5	Repetition rate(Hz)	100
Energy spread	5×10^{-3}		

For electron beams with energies close to $E_e = 260$ MeV ($\gamma \approx 520$), that, in collision with a laser with wavelength of about 1 μm ($E_{\mathrm{ph},L} = 1.2$ eV), produce Compton radiation with energy up to $E_{\mathrm{ph},r} = 4\gamma^2 E_{\mathrm{ph},L} \approx 1.2$ MeV (the energy in the center of mass of the two Compton photons being $\sqrt{s_{\gamma\gamma}} \lesssim 2.4$ MeV), the total Breit-Wheeler cross-section presents a broad peak at about 10^{-1} b just beyond the threshold at 1 MeV and not far from the $\gamma\gamma$ peak, but five orders of magnitude larger. In correspondence to this electron energy value, (where the electron-gamma energy in the center of mass is $\sqrt{s_{e\gamma}} \lesssim 36$ MeV) the TPP cross-section is more than one order of magnitude smaller than the Breit-Wheeler one, while the Compton at this same value of invariant mass and the Møller scattering (occurring at $\sqrt{s_{ee}} \approx 520$ MeV) will be discussed later.

The procedure of our analysis is therefore the following: first of all, on the basis of linac accelerated electron beams [18] and high energy lasers, we evaluate the emitted Compton radiation whose energy spectrum ranges between $E_{\mathrm{ph},L}$ and $E_{\mathrm{ph},r}$ [19]. Two counterpropagating twin Compton sources, whose interaction points have been placed at a distance $2L$ of few millimeters, are considered. The parameters of both beams are reported in Table I. These substantially reflect the ELI-NP-GBS [13] performances in single-bunch mode, so to avoid the use of laser recirculators or optical cavities which look incompatible with the clearance needed for BWPP or $\gamma\gamma$ event detection. The electron beam lines are similar to those shown in Ref. [14], with the difference that the electron energy is slightly larger (260 MeV, instead than 240) and, since the BW cross-section is five orders of magnitude larger than $\gamma\gamma$, the focusing is less demanding ($\sigma_x \approx 5$ μm, instead than 2 μm) and the focusing system much less critical. The radiation spectrum and energy distribution are presented in Fig. 4.

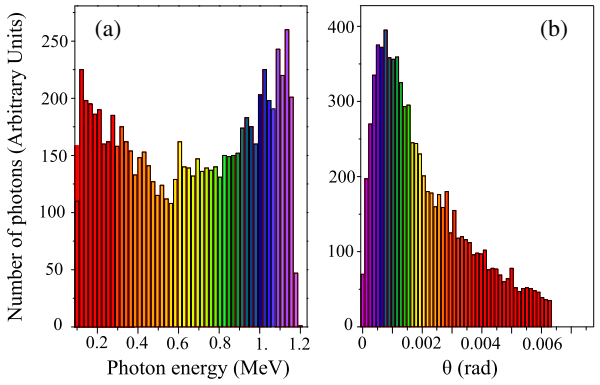

FIG. 4. Spectrum of the radiation (a) and angular distribution (b). Similar colors code similar groups of photons.

Due to the threshold at $\sqrt{s} = 2m_e$, only those photon couples with invariant mass $\sqrt{s} > 1.022$ MeV take part to BWPP. The Compton edge is at about $E_{\mathrm{ph},r} \approx 1.2$ MeV, therefore only photons with energies larger than 0.21 MeV can participate to the process. Due to the broad spectrum of the gamma rays, the collisions are in general not exactly symmetric, and a dispersion of the energy in the center of mass takes place, but, due to the Compton energy-angle correlation, the photons encounter preferably other photons with similar energy, and the number of asymmetric collisions is therefore quite contained. The $\gamma\gamma$ interaction region, distant L from each Compton interaction point, has transverse extension depending on the distance and on the divergence of the photons, that scales as the inverse of the electron Lorentz factor γ_e.

During the propagation of the photon beams a halo develops, due to the large spectrum of the gamma source and constituted mostly by photons with low energy under the BW threshold, and that do not contribute significantly to the interaction.

III. EVALUATION OF THE RATE OF EVENTS

We then evaluate the Breit-Wheeler pair production. The angular and energy distributions and the total number of pairs are calculated, the system being then optimized with respect to the pair flux orthogonal to the primary beam direction by varying the specifics of the electrons and the distance between the two Compton interaction points.

The particles (both electron and positrons) produced during the interaction as a function of energy E and zenithal angle θ in the laboratory frame are presented in Fig. 5, while their energy and angle distributions are in Fig. 6 for $2L = 8$ mm.

The angle distribution is symmetric with peaks at $\theta = 0.5$ and 2.6 rad. However, the number of particles emitted orthogonally with respect to the axis of the system is quite large, the distribution decreasing only by 20% with respect to the peak. The energy of the particles ranges between 0.5 and 1.3 MeV with a quite flat profile.

Figure 7 shows the total number of event for single shot as function of the distance between the two interaction points. The evaluation of the number of events per hour should take into account the repetition rate, that for a Compton source based on a room temperature single bunch operated rf linac achieves 100 Hz. With $L = 4$ mm, this number is about $N = 60$ event/h, allowing a good statistics.

All the calculations have been performed by using ROSE, a dynamical Monte Carlo code, implemented for studying

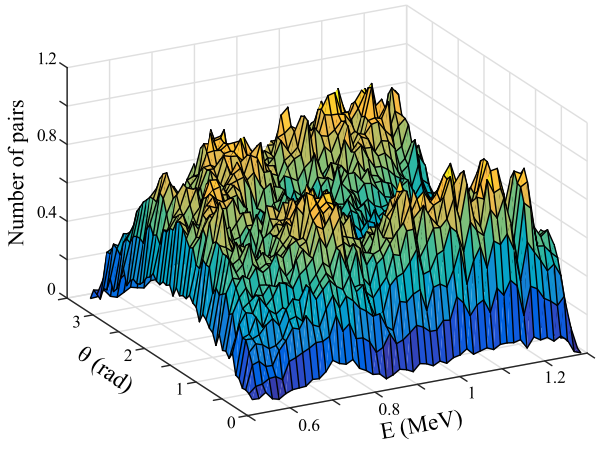

FIG. 5. Energy-angle BW pair distribution in the laboratory frame.

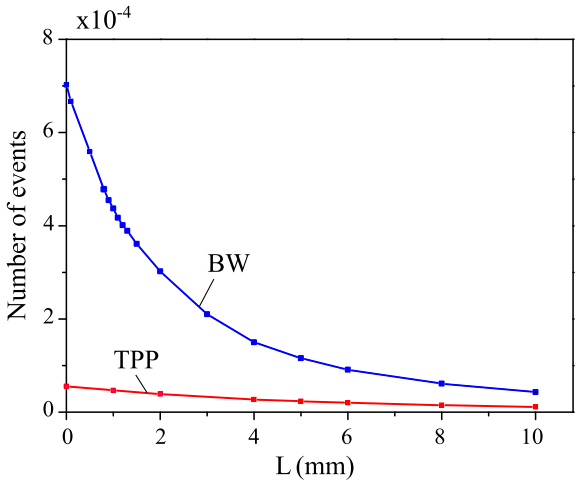

FIG. 7. Total number of BW (blue curve) and TPP events (red curve).

the photon-photon scattering and then extended to other collisions, as BWPP, TPP, Compton, and Møller scattering. Its main peculiarity is that it treats the scattering between two relativistic and realistic beams, following their time evolution in the laboratory frame. This is necessary whenever there is a significant spread in the invariant mass of the beam-beam collisions. Starting from two colliding beams of massive particles or photons (say beam 1 and beam 2) defined through the phase spaces of an appropriate number $N_{1,2}$ of macroparticles of weight respectively $q_{1,2}$, the procedure entails the definition of a common space grid where the kinematics takes place. The tracking of both beams during their overlapping up to the end of the scattering process permits us to dimension the total space window. The time evolution has been discretized over a total of N_T steps. At a certain time t, each ith ($i = 1, I$) cell contains $N_{1i}(t)$ and $N_{2i}(t)$ primary particles, forming $N_{c,i}(t) = N_{1i}N_{2i}$ pairs. The luminosity of the system is given by:

$$\mathcal{L}_i(t) = c(1+\beta)\frac{q_1 N_{1i} q_2 N_{2i}}{\Delta x_i \Delta y_i \Delta z_i} \tag{2}$$

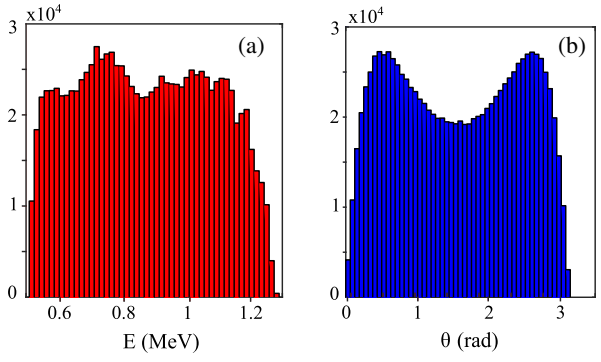

FIG. 6. Energy (a) and angular (b) BW pair distribution.

where Δx_i, Δy_i, and Δz_i are the transverse dimensions of the cells and $(1+\beta)$ is the relative velocity of the two beams. For each input couple, once that the output angles are randomly sampled in the center of mass reference frame, energies and momenta of the generated pair are evaluated, followed by a Monte Carlo procedure for accepting or rejecting the event on the basis of the value of the differential cross-section $d\sigma/d\Omega$ of the process. This last function must be given as a function of s and of the angle between $\underline{p}_1^{\mathrm{CM}}$ and $\underline{p}_4^{\mathrm{CM}}$ in the CM frame. The code, then, calculates the double differential rate of events for cell and time interval:

$$\frac{d^3 N_i(t)}{d\Omega dE dt} = \frac{d\sigma}{d\Omega dE}\mathcal{L}_i(t) \tag{3}$$

and, summing up on cells and integrating on time, the total angular distribution and, finally, the total number of events.

A Lorentz boost provides the angular and energy distributions of the pairs in the laboratory system. Typical values of the parameters of the calculation are $N_{1,2} = 30000$, $I = 100^3$, $N_T = 50$.

IV. CONSIDERATIONS ABOUT BACKGROUND

The background has then been evaluated considering the fact that the closest material elements in the proximity of the gamma-gamma interaction region (the detector, the electron final focusing system, and the laser mirrors) can be placed far enough from the IP in such a way that no Bethe-Heitler or trident processes are expected. Therefore, besides the photons scattered by $\gamma\gamma$ elastic collision ($\gamma\gamma \to \gamma\gamma$), the background is constituted by photons due to Compton ($e^-\gamma \to e^-\gamma$) and triplets ($e^-\gamma \to e^+e^-e^-$) generated by the primary electrons impinging the primary Compton gamma rays [20,21] and by the electrons of the Møller scattering ($e^-e^- \to e^-e^-$). The QED gamma-gamma events are

TABLE II. Number of events for single shot, $L = 4$ mm.

Event type	Breit-Wheeler	Compton	$\gamma\gamma$ pairs	Triplet pairs	Møller	Muon pairs
Number of event	1.6×10^{-4}	8×10^{-6}	$< 10^{-8}$	2.6×10^{-5}	1.5×10^{-6}	0

completely negligible due to the extremely low value of the total cross-section. As demonstrated in Refs. [14,15], in fact, they need a strong electron focusing at about 2–3 μm of transverse dimension, and, for not optimized cases, they are less than 1 event per hour. The other processes have been evaluated and compared in total number, energy, and angular distribution with respect to the BWPP process with the same ROSE code. As regards to the secondary Compton scattering, producing photons up to 260 MeV, the total cross-section at $\sqrt{s} = 36$ MeV is about 5 mb, almost two orders of magnitude lower than the BWPP's. Their total number is about 8×10^{-6} with the lower energy photons (1–2 MeV) spread all over the solid angle and the most energetic ones confined into a thin angle around the electron propagation axis. The TPP products have been computed by means of the cross-sections introduced in Refs. [20,21]. The total number of TPP particles is reported in Fig. 7, red curve. It is always smaller than the BW flux and, up to $L = 4$ mm, it maintains less than 15% of the BW.

As regards to the Møller scattering, since the differential cross-section is divergent on the axis, the evaluation of the total cross-section (Fig. 3) and of number and distribution of the events can be performed only by disregarding a cylinder around the primary beams, a region where the primary and the scattered electrons are not distinguishable and that cannot be covered by the detector.

The value of the Møller total cross-section reported in Fig. 3 (orange curve) has been evaluated by setting the cut at $\theta \leq 0.04$ rad. With this selection, that disregards a very thin region, the number of Møller events is still two orders of magnitude smaller than the BW one. Finally, the system is under the threshold of the muon photo-production. The number of events for all the processes is presented in Table 2.

V. CONCLUSIONS

Pike *et al.* have recently stressed the importance of detecting BW pairs from photon-photon collisions [11]. Here we have demonstrated that with state-of-the-art devices and with not particularly demanding parameters this process neatly emerges from the background of competing processes and can be easily detected. However, several critical points should be taken into account: the Compton backscattering production of high-energy photons, for instance, poses challenging endeavors connected to the focal stage of the electron beam, that is the closest material element to the gamma IP and must satisfy geometrical constraints. Other quite demanding requirements, the low emittances and energy spread of the electron beam, the necessity of 100 Hz of repetition rate, the high brilliance of the laser system, have been already extensively studied, tested and fulfilled in several previous beam dynamics experiments and projects. Strategies for separating the charged particles from photons based on the detection by electric or magnetic fields, or the development of geometries avoiding the direct collision between the electron beams and primary gammas, thus decreasing the triplet pair rate production should be analyzed. Also the detection system needs an *ad hoc* design, that can be based on the wide literature in the field. The photon-photon collider that we describe would also be controllable and flexible, permitting, in particular, the manipulation of photon polarization in a way that would allow extensive tests of the properties of the BW process. This collider would also be the first such facility, and it would open the way to further exciting developments.

I. D. and D. M. equally contributed to this work.

[1] G. Breit and J. A. Wheeler, Collision of two light quanta, Phys. Rev. **46**, 1087 (1934).

[2] F. D. Valle, A. Ejlli, U. Gastaldi, G. Messineo, E. Milotti, R. Pengo, G. Ruoso, and G. Zavattini, The PVLAS experiment: measuring vacuum magnetic birefringence and dichroism with a birefringent Fabry–Perot cavity, Eur. Phys. J. C **76**, 24 (2016).

[3] A. Cadène, P. Berceau, M. Fouché, R. Battesti, and C. Rizzo, Vacuum magnetic linear birefringence using pulsed fields: status of the BMV experiment, Eur. Phys. J. D **68**, 16 (2014).

[4] G. Jarlskog, Measurement of delbrück scattering and observation of photon splitting at high energies, Phys. Rev. D **8**, 3813 (1973).

[5] R. P. Mignani, V. Testa, D. G. Caniulef, R. Taverna, R. Turolla, S. Zane, and K. Wu, Evidence for vacuum birefringence from the first optical-polarimetry measurement of the isolated neutron star RX J1856.5-3754, Mon. Not. R. Astron. Soc. **465**, 492 (2017).

[6] C. Bamber *et al.*, Studies of nonlinear QED in collisions of 46.6 GeV electrons with intense laser pulses, Phys. Rev. D **60**, 092004 (1999).

[7] C. Gahn, G. D. Tsakiris, G. Pretzler, K. J. Witte, C. Delfin, C.-G. Wahlström, and D. Habs, Generating positrons with femtosecond-laser pulses, Appl. Phys. Lett. **77**, 2662 2664 (2000).

[8] H. Chen, S. C. Wilks, J. D. Bonlie, E. P. Liang, J. Myatt, D. F. Price, D. D. Meyerhofer, and P. Beiersdorfer, Relativistic Positron Creation Using Ultraintense Short Pulse Lasers, Phys. Rev. Lett. **102**, 105001 (2009).

[9] K. Homma, K. Matsuura, and K. Nakajima, Testing helicity-dependent $\gamma\gamma \to \gamma\gamma$ scattering in the region of MeV, Prog. Theor. Exp. Phys. **2016**, 013C01 (2016).

[10] X. Ribeyre, E. d'Humières, O. Jansen, S. Jequier, V. T. Tikhonchuk, and M. Lobet, Pair creation in collision of γ-ray beams produced with high-intensity lasers, Phys. Rev. E **93**, 013201 (2016).

[11] O. J. Pike, F. Mackenroth, E. G. Hill, and S. J. Rose, A photon–photon collider in a vacuum hohlraum, Nat. Photonics **8**, 434 (2014).

[12] D. Burke *et al.*, Positron Production in Multiphoton Light-by-Light Scattering, Phys. Rev. Lett. **79**, 1626 (1997).

[13] O. Adriani *et al.*, Technical Design Report EuroGammaS proposal for the ELI-NP Gamma beam System, arXiv: 1407.3669v1.

[14] D. Micieli, I. Drebot, A. Bacci, E. Milotti, V. Petrillo, M. R. Conti, A. R. Rossi, E. Tassi, and L. Serafini, Compton sources for the observation of elastic photon-photon scattering events, Phys. Rev. Accel. Beams **19**, 093401 (2016).

[15] I. Drebot, A. Bacci, D. Micieli, E. Milotti, V. Petrillo, M. R. Conti, A. R. Rossi, E. Tassi, and L. Serafini, Study of photon–photon scattering events, Nucl. Instrum. Methods Phys. Res., Sect. A, DOI: 10.1016/j.nima.2016.07.039 (2016).

[16] K. Yokoya, https://ilc.kek.jp/~yokoya/CAIN/Cain242/CainMan242.pdf.

[17] I. Drebot *et al.*, ROSE: A numerical tool for the study of scattering events between photons and charged particles, Nucl. Instrum. Methods Phys. Res., Sect. B, DOI: 10.1016/j.nimb.2017.02.076 (2016).

[18] A. Bacci *et al.*, Electron Linac design to drive bright Compton back-scattering gamma-ray sources, J. Appl. Phys. **113**, 194508 (2013).

[19] V. Petrillo *et al.*, Polarization of x-gamma radiation produced by a Thomson and Compton inverse scattering, Phys. Rev. ST Accel. Beams **18**, 110701 (2015).

[20] E. Haug, Bremsstrahlung and pair production in the field of free electrons, Zeitschrift für Naturforschung A **30a**, 1099 (1975).

[21] E. Haug, Simple Analytic Expressions for the Total Cross Section for y-e Pair Production, Zeitschrift für Naturforschung A **36a**, 413 (1981).